Radial lip seals, thermal aspects

Paper III(iv)

Radial lip seals, thermal aspects

M. J. L. Stakenborg and R. A. J. van Ostayen

In this paper the influence of temperature on the seal-shaft contact is studied, using coupled temperature-stress FEM analysis. A thermal network model is used to calculate the seal-shaft contact temperature for steady-state and transient conditions. Contact temperatures were measured under the seal lip, employing different measurement techniques. The experimental and numerical results show good correspondence. This study demonstrates that the thermal network theory provides a useful tool to predict the seal-shaft contact temperature.

Nomenclature

b	Contact width	[m]
c	specific heat	[J/kgK]
h	Film coefficient for convection	[W/m^{2}K]
p_0	Static contact pressure	[Pa]
t	Time	[s]
C_1, C_2	Mooney constants	[Pa]
F_r	Radial contact force	[N]
Q_i	Heat flow i	[W]
R_i	Heat resistor i	[K/W]
T	Torque	[Nm]
T	Temperature	[°C]
α	Thermal expansion coefficient	[1/K]
η	Dynamic viscosity	[Pa.s]
λ	Thermal conductivity	[W/mK]
ρ	Specific mass	[kg.m^{-3}]
ω_1	Shaft angular velocity	[rad.s^{-1}]
ω_2	Seal angular velocity	[rad.s^{-1}]

1 INTRODUCTION

The friction heat generated in the seal-shaft interface results in a raise in seal temperature . Investigating the sealing mechanism of radial lip seals it is important to know the influence of temperature on the contact conditions such as contact force, contact width and contact stress distribution, because they are the boundary conditions for the sealing and lubrication mechanism.
In the first part of this paper the influence of temperature on the seal-shaft contact force is studied, for a standard Nitrile rubber radial lip seal of Nitrile with industrial code BAF 100*10*70, to be used on a shaft diameter of 70mm.
With respect to service life, the seal application engineer needs an indication of the seal-shaft contact temperature which will occur in the seal in practice. In the second part of this paper a thermal network model is employed to calculate the contact temperature. Further, 3 different experimental techniques are utilized to measure the contact temperature.
Finally the numerical results are compared to the experimental results.

2 TEMPERATURE EFFECTS

A distinction can be made between (a) irreversible and (b) reversible temperature effects on the contact conditions. Some examples of irreversible temperature effects are :

1) Influence of temperature on physical ageing, resulting in a permanent change in stiffness of the rubber.
2) Influence of temperature on chemical ageing due to chemical reactions between oil (-additives) and rubber.
3) Influence of temperature on swell of the rubber due to absorbtion of oil (-additives).

The irreversible temperature effects will not be discussed in detail. In this paper we will confine ourselves to the following reversible temperature effects :

1) Influence of temperature on the stiffness of the rubber.
2) Influence of the temperature on the stiffness and initial length of the garter spring.
3) Thermal expansion of the seal material.
4) Thermal expansion of the shaft.

To study the influence of these reversible temperature effects on the contact conditions, information is needed on the temperature distribution in the seal.
In principle the temperature distribution in the seal can be determined in a number of

different ways, e.g. by analytical models [1], by the finite difference method [5], by the boundary element method [10], or by the finite element method [6]. In this paper the finite element method was chosen because this method allows a coupled stress-temperature analysis.

3 TEMPERATURE DISTRIBUTION IN THE SEAL

In this paragraph the temperature distribution in the seal is discussed. In the next paragraph the influence of the temperature distribution on the contact conditions is investigated.
In [9] it is shown that isothermal FEM calculations of the contact force of a Nitrile rubber lip seal using the Mooney-Rivlin material model showed very good correspondence with experimental contact force measurements on a split shaft device. A coupled stress-temperature FEM analysis was performed, assuming that the stress is dependent on the temperature distribution, but that there is no inverse dependence. The thermal stresses only had a very minor influence on the deformed shape of the seal. Therefore it was assumed that the temperature distrubution was not dependent on the stresses. The temperature distribution was calculated using the deformed seal geometry for isothermal conditions at T = 30 °C, see [9]. The calculated temperature field was then used as an input for the coupled stress-temperature analysis. In the coupled analysis the 2 Mooney-Rivlin constants depend on temperature.
The heat problem was assumed to be axisymmetric and the ABAQUS FEM model [12] contained 676 4-node, linear, axisymmetric ring, heat transfer elements. The garter spring and the metallic case were given the thermophysical properties of steel. It was assumed that the thermophysical material properties and the convective boundary conditions are not temperature dependent, thus the heat analysis problem was assumed to be linear. Note however that the stress/strain analysis of the contact problem remains nonlinear.
See table 1 for the (thermo-) physical properties of Nitrile rubber and steel. The following thermal boundary conditions were prescribed on boundaries Γ_1, Γ_2, Γ_3 and Γ_4 (see fig 1) :

1) Γ_1 : Fixed temperature T_m where the seal is in contact with the machine housing.
2) Γ_2 : Fixed temperature T_c in the seal-shaft contact area.
3) Γ_3 : Convection to oil on oilside of the seal, for oil bulk temperature T_{oil} and film coefficient h_{oil}.
4) Γ_4 : Convection to air on airside of the seal, for air temperature T_{air} and film coefficient h_{air}.

The steady-state temperature distribution in the seal was calculated for 5 different sets of boundary conditions as represented in table 2. Figure 1 shows the steady-state temperature distribution in a seal calculated with the FEM model for case 5 of table 2. With case 2 as initial condition the steady-state temperature distribution was reached after a transient time of 25 minutes.
The values of film coefficients h_{air} and h_{oil} are estimates based on formulae given in [2].

4 INFLUENCE OF TEMPERATURE ON THE CONTACT CONDITIONS

The influence of the 4 reversible temperature effects on the contact force for the 5 cases of table 2 is summarized in figure 2. Case 2 was chosen as the starting or reference situation.
Figure 3 shows the E-modulus determined from (quasi-)static iso-thermal uni-axial stress-relaxation tests on Nitrile rubber specimen. Using these experimental data the Mooney constants C_1 and C_2 were determined as function of the temperature. The (reversible) influence of the temperature on the seal material stiffness results in a change in contact force as represented in column 1 of figure 2. The stiffness of the garter spring and its initial length are both a function of temperature. The influence of this temperature effect on the contact force is shown in column 2 . The influence of thermal expansion of Nitrile rubber on the contact force is shown in column 3. Column 4 shows the influence of thermal expansion of the shaft on the contact force. Column 5 shows the influence of the 4 effects together. With 10 nodes (9 elements) in the contact width (b=0.075 mm) no change in contact width was found for all 5 cases, and only very minor changes in contact stress distribution occurred.

5 DISCUSSION OF THE FEM RESULTS

The influence of the temperature on the contact conditions is relatively small for the 5 cases described above. It is worthwhile to consider that :

1) It is the aim of the seal manufacturer to produce a seal that is not very sensitive to changes in temperature. Thus a rubber is chosen which stiffness is not very temperature dependent. In addition the garter spring has received a special temperature treatment to reduce the influence of temperature on the spring stiffness.

2) Only a relatively small zone in the tip of the seal is exposed to higher temperatures, see figure 1.

3) In practice contact temperatures higher than T_c=100 °C of case 5 will often occur. These higher temperatures were not taken into account in the FEM analysis. For temperatures beyond 100 °C the rubber stiffness rapidly changed due to physical ageing (additional vulcanisation), resulting in an irreversible change of rubber stiffness.

4) Although the influence of temperature on the static stiffness is small, temperature can have a strong influence on the dynamic rubber stiffness. This dynamic stiffness may become important in case of periodic excitation of the seal lip due to eccentric movements of the shaft center, or due to out-of-roundness of the shaft, see [9].

It is recommended by seal manufacturers not to use lip seals beyond a certain maximum operating temperature, depending on the composition of the seal material (for Nitrile rubber $T_{max} \approx 90$ °C). Beyond this temperature increased wear will occur, resulting in a considerable decrease in seal service life. The contact temperature which results from a certain dissipated friction heat depends on the heat balance in the entire machine. In the next paragraph a numerical method is presented to calculate an estimate of the steady-state and transient contact temperatures.

6 THERMAL NETWORK METHOD.

In the thermal network method (TNM) a machine is divided into thermal components, forming a thermal network.
The thermal components used in such a network are resistances, capacitors, and positive and negative heat sources. In analogy with electrical circuits, temperature corresponds to voltage and heat rate to current.
Advantages of the TNM method for thermal analysis are : (a) the TNM is easy to conceive and very flexible because of its open structure and (b) the TNM does not demand sophisticated software and hardware. The TNM calculations presented in this paper can be performed on a simple (640 kilobyte) personal computer.
Nevertheless, this method has not yet been used frequently for the analysis of heat problems in mechanical engineering. The main reason is that there are often no adequate analytical models available to describe the different mechanical elements such as gears, bearings and seals in terms of thermal components such as resistances, capacities or heat sources.
The FEM is frequently used for analysing heat problems in mechanical engineering. A disadvantage of the FEM in comparison with the TNM is that the software and hardware are expensive.

In the present paper a combined approach was chosen. The FEM can be used to determine thermal conductivity matrices for relatively complex machine elements, such as seals. These conductivity matrices are then incorporated into the thermal network model.
The size of the conductivity matrix of a machine element depends on the number of temperatures and heat fluxes one wishes to distinguish for that element. The heat flow and the temperature distribution in the seal are assumed to depend on only 4 temperatures: (1) the seal-shaft contact temperature, (2) the temperature of the machine housing, (3) the bulk oil temperature, and (4) the air temperature. Hence, the conductivity matrix of the seal is a 4x4 matrix. This reduces the original 676 element FEM-mesh of the seal to a simple, condensed and more efficient network component.
The thermal network model of the test-rig from figure 4 is shown in figure 5, see also van Ostayen [4]. A part of the test-rig on the lefthand side of the shaft was modelled by one resistor and one capacitor only. The thermal resitance and capacity of these two components have been derived from measurements. This simplification is allowed here, because we are mainly concerned with the relation between the dissipated heat and the temperature in the seal-shaft contact area. The resulting network is smaller and machine elements such as the slip ring unit and the rotating air bearings do not have to be modeled.

The oilfilm between seal and shaft is assumed to have one homogeneous temperature. One node n_0 therefore suffices to describe the oilfilm, see fig. 6. This node is connected to the following components :

1) A heat source Q_0 describing the heat flow dissipated to the oilfilm.
2) A resistor R_1 related to the conductive heat transfer from the oilfilm to the seal. The oil flow in the oilfilm is assumed to be laminar. Then the heat transport from the oilfilm to the seal is conductive and perpendicular to the laminar flow.
3) A resistor R_2 related to the conductive heat transfer from the oilfilm to the shaft.
4) A resistor R_3 related to the heat transfer from the oilfilm to the bulk oil. A part of the heated oil in the oilfilm will be exchanged with the cooler bulk oil. The result is a heat flow from the oilfilm to the oil bulk.

The shaft under the seal is modeled by 82 resistors and 31 capacitors thus enabling a good representation of the large radial and axial temperature gradients. For reasons of simplicity a reduced number of resistors and capacitors are sketched in the shaft of fig. 5.

The other metal elements in the rig such as the oil container and the static air bearing are modeled with less resistors and capacitors because of the very small temperature gradients within these elements. Heat transfer by convection is calculated using the formulae from [2]. Generally these formulae are nonlinear in temperature.

The nonlinear system equations of the thermal network were solved using a standard network program mainly used by electronical engineers: SPICE-2G. It is a general purpose circuit simulation program for steady-state or transient nonlinear analysis. Circuits may contain resistors, capacitors, independent and dependent voltage and current sources and several other electrical components. Nonlinear functions however are limited to polynomials.

7 CONTACT TEMPERATURE MEASUREMENTS

Because of the relatively small dimensions of the contact width b (in practice $0.05 < b < 0.5$ mm) it is difficult to measure the contact temperature. Different experimental methods were employed to measure the contact temperature distribution.

1) NTC thermistors.
2) Thin film thermal transducers.
3) Infra-red temperature measurements.

NTC thermistors are reliable, relatively inexpensive, commercially available temperature sensors (accuracy +/- 1 °C). A disadvantage of these thermistors is that because of their diameter (d = 2 mm) only an average contact temperature can be measured in a bandwidth which is much larger than the actual contact width.
Therefore, attempts were made to use a Titanium thin film micro-transducer, which was evaporated on the shaft surface, see figure 7. Because of the small dimensions of these sensors (width = 10 μm, length = 600 μm, height = 1 μm) and their accuracy (+/- 0.5 °C) they seemed very useful for measuring the contact temperature (distribution) under the lip. In order to measure the temperature profile in the contact area the seal was translated in axial direction over the transducer on a rotating shaft. Problem here was that each time the seal was translated, the torque changed, probably because the seal encountered a different local roughness pattern on the shaft, which resulted in a change of dissipated friction heat and in small fluctuations of the contact temperature of +/- 2 °C. This temperature fluctuation was too large to obtain a valid temperature profile within the contact area. Disadvantages of these micro-transducers sensors are (a) that due to wear they have a limited service life (approximately 2 hours) which is short compared to the transient times before the contact temperature has reached a steady state (approximately 1.5 hours), and (b) that the shaft surface had to be polished (locally) before evaporation, resulting in a local change of shaft roughness, and thus in a change of torque.

In order to obtain an integral temperature profile of the contact temperature of the seal lip contact surface, infra-red temperature measurements were performed via a mirror and a small cylindrical glass window (diameter = 2 mm, length = 1 mm), in a fixed hollow steel shaft. The temperature profile measured at 3 different seal angular velocities is represented in figure 9. The infra-red measurement technique is based on determining temperature differences (resolution 0.5 °C). However, an accurate determination of the absolute temperature is difficult with this technique without a reference temperature.

8 NUMERICAL RESULTS

The results are valid for the test-rig of figure 4, where the non-rotating shaft was immersed in Shell Tellus 46 oil, over an angle of 0.68 rad of the shaft circumference. The ambient air temperature was held constant at T = 20 °C.

The torque was measured as function of the shaft angular velocity, see fig 10. Figure 11 shows the steady-state contact temperatures measured with the thermistors, corresponding to the torque of figure 10. In the same figure are sketched the steady-state contact temperatures as calculated with the TNM, for 2 situations : (a) with the seal taken into account and (b) without the seal taken into account in the network model.
In situation (a) the seal was incorporated into the TNM as a 4x4 conductivity matrix as determined by the FEM. This results in a heat flow as represented in figure 12.
In situation (b) the heat transfer through the seal was eliminated by giving the seal a very high resistance (if $R_1 = \infty$ then $Q_1 = 0$). From figure 11 it can be seen that the presence of the seal as a thermal component has only a very minor influence on the calculated contact temperatures. Therefore it can be concluded that the seal does not necessarily have to be taken into account in the network. This simplification eliminates the use of the FEM analysis to determine the seal conductivity matrix, which means a considerable reduction in modeling time.
Figure 13 shows transient contact temperatures at a constant shaft angular velocity for situation (b).
The practical utility of the TNM is illustrated by the good correspondence between measured and calculated results for both steady-state and transient situations.

9 SUMMARY

1) For the Nitrile rubber lip seal under investigation, the influence of the contact temperature T_c on the static contact conditions is neglectably small for $0<T_c<100$ ^oC.
2) To calculate the seal-shaft contact temperature resulting from a certain dissipated friction heat rate the heat balance of the entire machine has to be taken into account.
3) The thermal network method provides a useful tool to model the heat balance of the machine and to calculate transient and steady-state seal-shaft contact temperatures.
4) The heat transfer through the seal has only a very minor influence on the contact temperature.
5) Accurate experimental determination of the contact temperature is difficult due to the small dimensions of the seal-shaft contact width.

10 ACKNOWLEDGEMENT

The author would like to thank Mr. B. Munneken from the CFT Department of Philips Eindhoven for performing the infra-red temperature measurements.

References

[1] Upper,G. "Dichtlippentemperatur von Radial-Wellen Dichtringen", Thesis University of Karlsruhe, Germany, July 1967.(In German)

[2] Wong, H.Y. "Handbook of essential formulae and data on heat transfer for engineers", Longman, London and New York, 1977.

[3] van Leeuwen, H; Meyer, H; Schouten, M.J.W. "Elastohydrodynamic film thickness and temperature measurements in dynamically loaded concentrated contacts: eccentric cam-flat follower", Proc. 13th Leeds-Lyon Symposium on Tribology, University of Leeds, 8-12 sept. 1986.

[4] van Ostayen, R.A.J. "The use of the thermal network method for modeling the heat balance in mechanical constructions", M.Sc. Thesis, Eindhoven University of technology, August 1988.(in Dutch)

[5] Ozisik, M.N. "Heat Transfer, a Basic Approach", Mc Graw-Hill Book Company, New York 1985.

[6] Bathe, K.J. "Finite Element Procedures in Engineering Analysis", Prentice-Hall, Inc., Englewood Cliffs, New Jersey, 1982.

[7] ten Hagen, E.A.M., "Mechanical Characterization of Synthetic Rubbers" , M.Sc. Thesis, Eindhoven University of Technology, Jan. 1988.(in Dutch)

[8] Treolar, L.R.G. "The physics of rubber elasticity", Clarendon Press, Oxford, 1975.

[9] Stakenborg, M.J.L.,"On the sealing and lubrication mechanism of radial lip seals", Ph.D. Thesis, Eindhoven University of Technology, the Netherlands. Sept. 1988.

[10] Brebbia, C.A. "Applications of the boundary element method for heat transfer problems", Rev. Gen. Therm. Fr. no 280, April 1985.

[11] Luyten, R. "Determination of the contact force, contact width and the contact stress distribution of radial lip seals.", M.Sc. Thesis, Eindhoven Univ. of Techn., Dec 1987.(in Dutch)

[12] Hibbit, Karlson and Sorensen ABAQUS FEM software, user manuals (version 4-5)

		Nitrile	Steel
Specific mass	ρ [kg.m^{-3}]	1460.	7800.
Thermal conductivity	λ [W/mK]	.43	50.
Specific heat	c [J/kgK]	2000.	450.
Thermal expansion coeff.	α [1/K]	9.44 10^{-5}	1.1 10^{-5}

Table 1 : Thermo-physical properties of Nitrile rubber and steel.

case	T_c [°C]	T_{air} [°C]	T_{oil} [°C]	T_m [°C]	h_{air} [W/m^{2}K]	h_{oil} [W/m^{2}K]
1	0.	0.	0.	0.	0.	0.
2	20.	20.	20.	20.	0.	0.
3	50.	20.	30.	20.	10.	200.
4	75.	20.	35.	20.	10.	200.
5	100.	20.	40.	30.	10.	200.

Table 2 : Thermal boundary conditions for 5 cases.

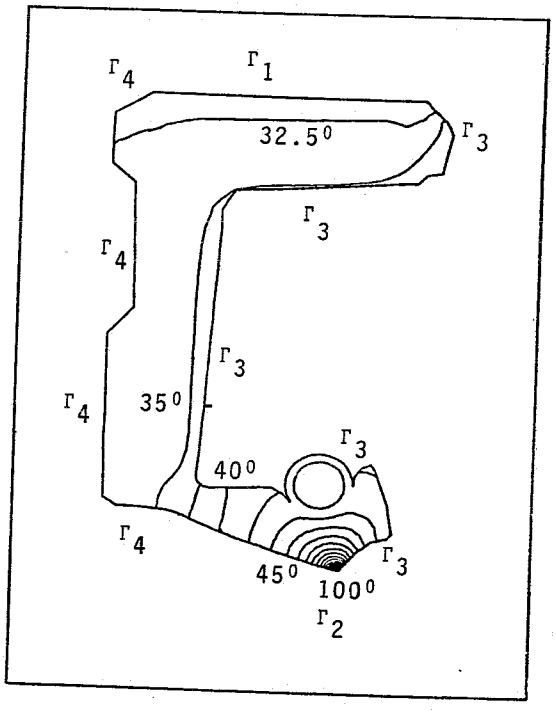

Fig. 1 : Steady-state temperature distribution in the radial lip seal of Nitrile rubber, calculated with the finite element method, for case 5 of table 2.

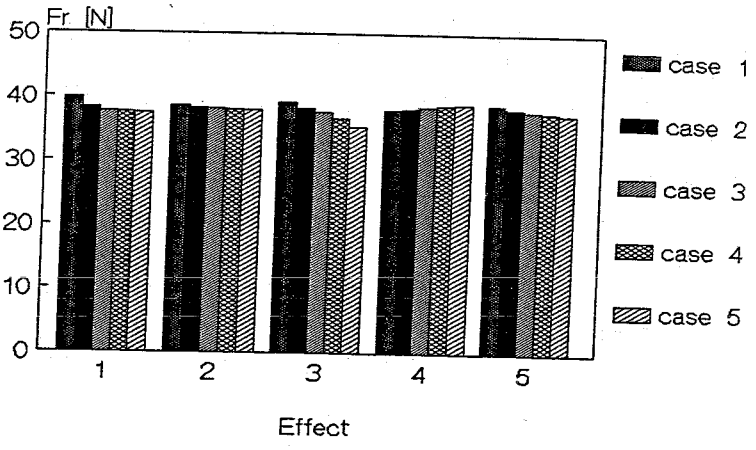

Fig. 2 : The contact force F_r for the 5 different cases of table 2 and for 5 effects, calculated by a coupled stress-temperature FEM analysis. The effects are :

1 Influence of temperature on material stiffness.
2 Influence of temperature on spring stiffness.
3 Influence of thermal expansion of the rubber.
4 Influence of thermal expansion of the steel shaft.
5 Combined effect of 1), 2), 3) and 4).

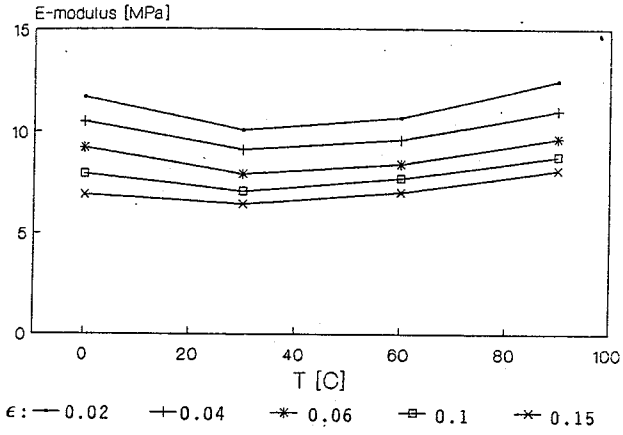

Fig. 3 : E-modulus of Nitrile rubber as function of temperature for different strains $\varepsilon = \Delta l/l$ after a relaxation time t=24 h.

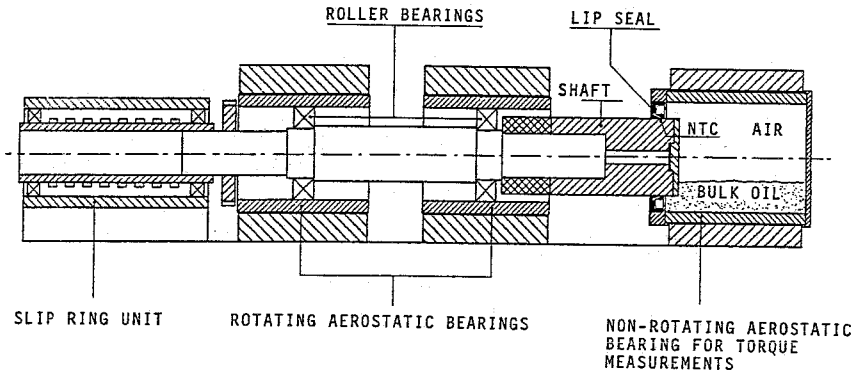

Fig. 4 : Sketch of temperature measurement test-rig .

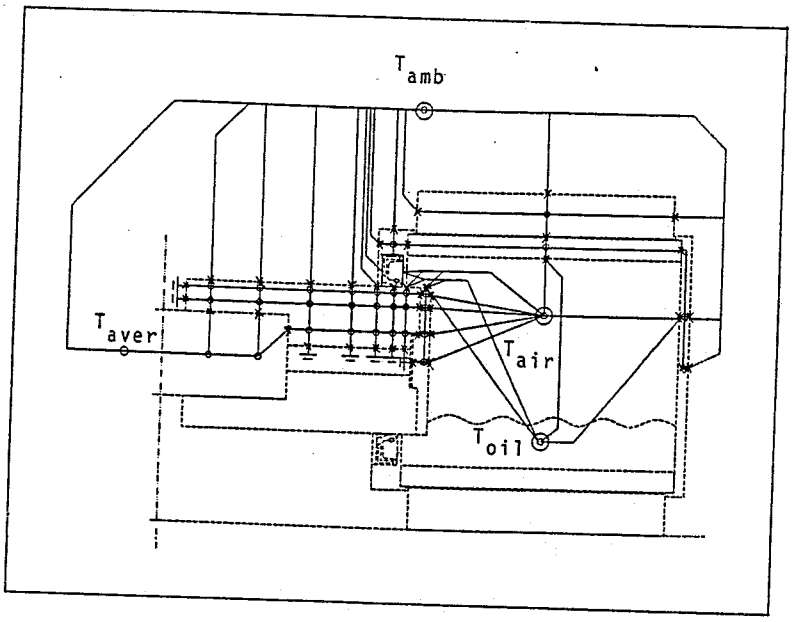

Fig. 5 : Thermal network model of the test-rig from fig. 4

o temperature node with capacity
x temperature node without capacity
___ each line connecting nodes represents a resistor.

T_{amb} this node represents the ambient air surrounding the test-rig, it is assumed to be constant at 20 °C.
T_{oil} this node represents the average oil bulk temperature.
T_{air} this node represents the average air temperature inside the housing.
T_{aver} this node represents the average temperature of the part of the test-rig that was not modeled: the slip ring unit, the rotating aerostatic bearings and the main shaft.

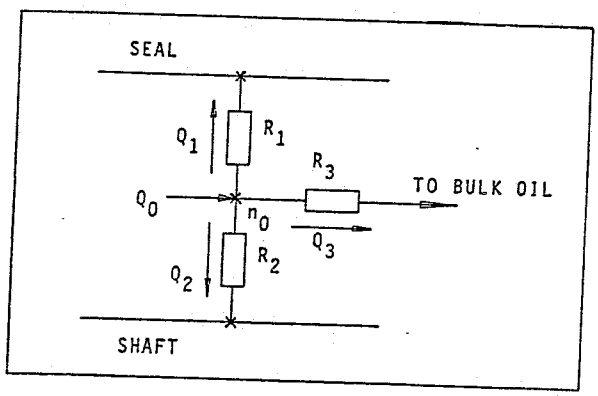

Fig. 6 : Detail of thermal network in the contact area.

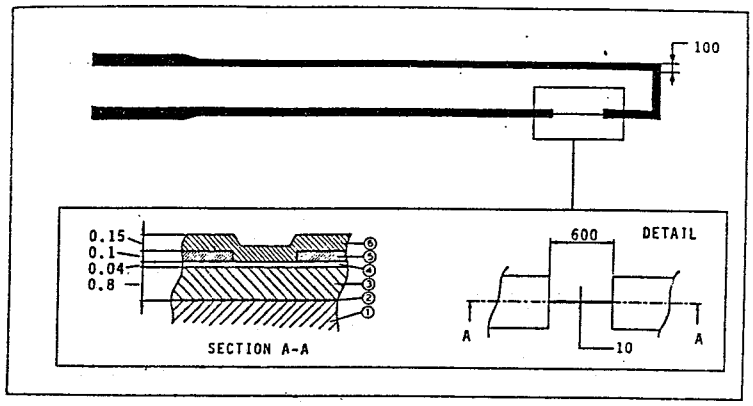

Fig. 7 : Thin film thermal microtransducer (dimensions are in microns). (1) substrate (shaft), (2) adhesive layer of Ti, (3) insulating layer of Al_2O_3, (4) transducer of Ti, (5) conductor pattern of Au, (6) protective layer of Al_2O_3, see [3].

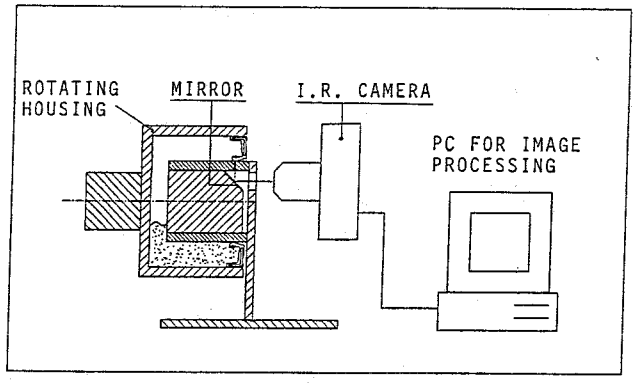

Fig. 8 : Sketch of test-rig for infra-red temperature measurements.

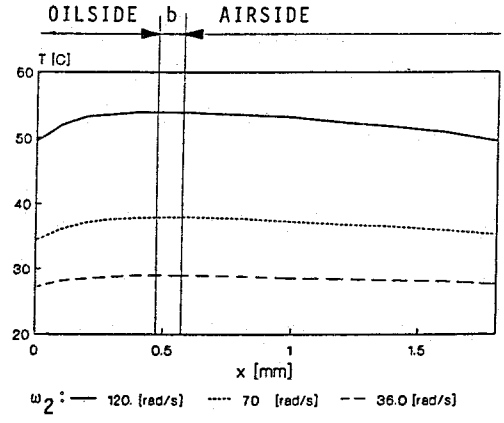

Fig. 9 : Temperature distribution for different seal angular velocities, measured using the infra-red technique.

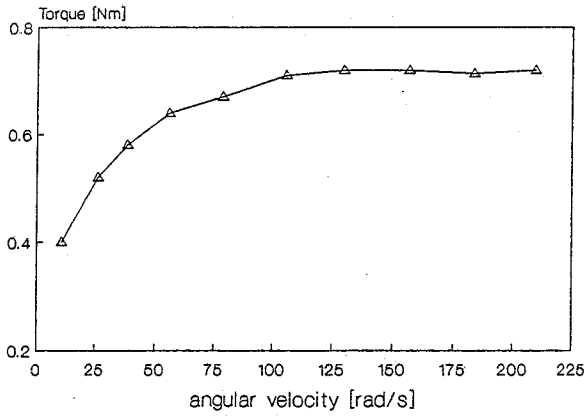

Fig. 10 : Steady-state seal torque as function of the shaft angular velocity as measured on the test-rig.

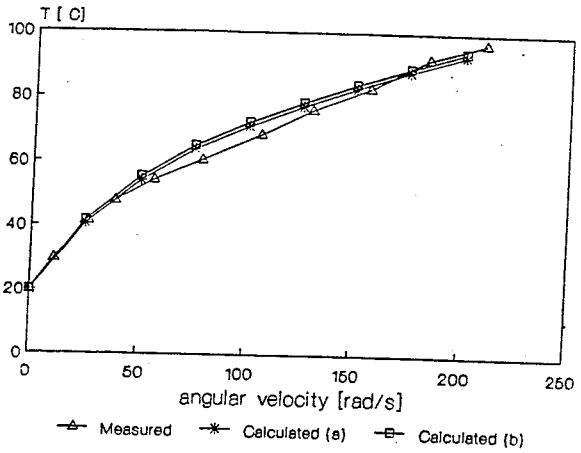

Fig. 11 : Steady-state seal-shaft contact temperature as function of the shaft angular velocity corresponding to seal torque in fig. 10.

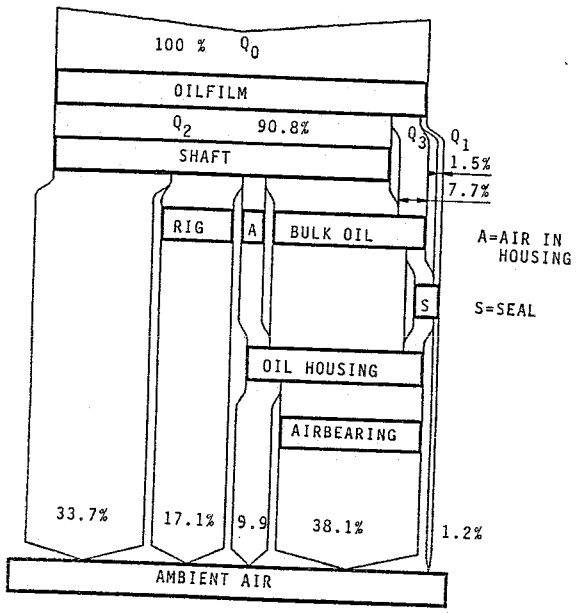

Fig. 12 : Sankey-diagram of the heat flows in the test-rig as calculated with the TNM. ω = 125 rad/s and T = 0.72 Nm, thus $Q_0 = T.\omega$ = 90 W.

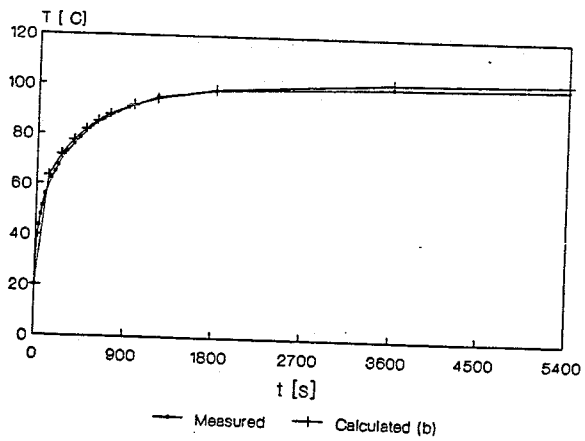

Fig. 13 : Transient contact temperatures for ω = 204.2 rad/s and a steady-state torque T = 0.82 Nm. The steady-state torque was reached after 900 seconds.